Measurement of tZq differential cross-section

Dissertation
zur
Erlangung des Doktorgrades (Dr. rer. nat.)
der
Mathematisch-Naturwissenschaftlichen Fakultät
der
Rheinischen Friedrich-Wilhelms-Universität Bonn

vorgelegt von
Nilima Akolkar
aus
Vadodara, India

Bonn 2023

Angefertigt mit Genehmigung der Mathematisch-Naturwissenschaftlichen Fakultät der Rheinischen Friedrich-Wilhelms-Universität Bonn

1. Gutachter: Prof. Dr. John Smith
2. Gutachterin: Prof. Dr. Anne Jones

Tag der Promotion:
Erscheinungsjahr:

Contents

Todo list

CHAPTER 1

Theoretical Concepts and Experimental Basics

Since many years, physical phenomena occuring around us has shaped our understanding about nature. The Standard Model (SM) of particle physics is a theory that explains almost everything that nature has to offer. It is based on fundamental particles and their interactions being governed by Quantum Field Theories (QFTs).

The Standard Model is divided into spin-1 fermions and spin-0 bosons. The fermions are further divided into leptons and quarks as shown in FIGURE . Another classification of fermions is into generations. The first generation consstitutes u, d, e^- and ν_e which give rise to matter around us. The second and third generation particles are high energy *siblings* of the first generation particles. These are observed at high energies such as colliders. The SM also considers anti-particles which are clones of particles with opposite quantum numbers.

Add figure

These fermions interact with each other via exchanging bosons which are also called *force-carrier* particles. The massless neutral photon (γ) is the messenger of the electromagnetic (EM) force which is experienced by charged particles. The underlying QFT is called Quantum Electrodynamices (QED). The electrostatic attraction between charged particles is the low-energy manifestation of QED. Among the SM, all fermions except neutrinos are sensitive to the EM force. The underlying symmetry is the U(1) symmetry.

The strong interaction, mediated by massless gluons, is experienced by particles carrying the so-called colour charge. The physics behind the strong interaction is explained in Quantum Chromodynamics (QCD). Only the quarks can interact via the strong interaction. A peculiar thing in QCD is that the gluons themselves also carry colour charge.

The weak force carriers are $W^{\pm}$ and Z, which unlike γ and gluons, are massive and charged in case of $W^{\pm}$. The weak interaction manifests itself in phenomena such as, β-decay and fusion processes inside the sun. All the SM particles, including the neutrinoes, can feel the weak force. Before discussing the elecroweak unification, let's dive into the weak interaction. The interaction mediated by $W^{\pm}$ and Z is called charged-current weak interaction and neutral-current weak interaction, respectively. The famous Wu experiment proved that the charged current weak interaction violates parity. The parity violating nature of the weak interaction suggests that the interaction vertex must be different from that of QED and QCD. The weak interaction is described using a $V - A$ vertex and this fact imples that only left-handed chiral particle states and right-handed chiral antiparticle states can participate in charged-current weak interaction.

The last piece of the SM puzzle is the Higgs boson which is a spin-0 boson. All the particles gain

their mass by Higgs mechanism.

1.0.1 Feynman diagrams

Interactions between the SM particles can give rise to various processes. In order to visualise it, a tool called Feynman diagrams is widely used. These diagrams are pictorial representations of the interactions which makes use of straight lines with arrows to show particles and anti-particles. Moreover, curly lines are used to show the boson exchanged between them. The Feynman diagrams are symbolic and have no physical meaning.

Add and explain an example feynman diagram

Explain matrix element, cross section and differential cross-section calculation

1.1 The Strong Force

Electrons and nucleus inside an atom are held together by the electromagnetic force. The same force also exists between protons inside the nucleus causing repulsion. However, there exists a force which is strong enough to overcome repulsion and keep the nucleus together. It is called the strong force or the strong nuclear force. The QFT describing the strong force is called Quantum Chromodynamics (QCD) and the underlying symmetry group is SU(3) described by 3×3 matrices. The eight generators of the SU(3) group give rise to eight gluons which are the strong force mediators. The structure of the SU(3) group demands that the wave function of the strongely interacting particle must be a 3-component vector. This gives rise to a new degree of freedom called "colour", with three states called red,blue and green. Consequently, particles having a non-zero colour charge can feel the strong force. Among the SM particles, only quarks have the colour charge which can be either red, blue or green.

A major differentiating factor between QCD and QED is that the gauge boson in QCD carries the charge of interaction. In other words, gluons also carry the colour charge which allows them to interact with other gluons as well. As a result of this self-interaction, no coloured object can be found as a free particle in nature. Due to this so-called colour confinement, quarks cannot exist independently but instead are found in colour-neutral states called *hadrons*. For instance, if two quarks are pulled away from each other, a gluon field is created between them which is proportional to the separation. The gluon fields is so strong that at some point, the energy in this field is sufficient to produce new quarks and antiquarks that form colourless bound states. This process is called hadronisation. Due to colour confinement, only certain configurations for hadrons are permitted. The possible combinations discovered so far can be categorised into mesons ($q\,\overline{q}$), baryons ($q\,q\,q$) and antibaryons ($\overline{q}\,\overline{q}\,\overline{q}$).

1.2 The Electroweak theory

In the 1960s, physicists were trying to formulate a gauge theory for weak interactions similar to QED. A theory can be a gauge theory if it has an underlying mathematical symmetry and it is renormalisable[1]. Glashow, Salam and Weinberg discovered such a gauge theory by unifying electromagnetic force and the weak force.

[1] A quantum field theory is renormalisable if...

The electroweak (EW) theory is a unification of QED and the thoery of weak interactions. It is described by the symmetry group $SU(2)_L \otimes U(1)_Y$. The corresponding charges of the electroweak theory are the weak isospin I, I_3 and the weak hypercharge Y. The weak hypercharge Y determines the interaction under the $U(1)$ transformations. The weak isospin of particles determines their transformation under $SU(2)$ and therefore, it is used to make multiplets of particles. The left-handed leptons (ℓ_L) will form doublets as shown in EQUATION because they transform into each other under the influence of weak force. This is due to to the $V-A$ vertex form of the weak interaction. On the other hand, the right-handed particles are singlets(ℓ_R).

fix the format and label reference

$$\ell_R = e^-_R, \mu^-_R, \tau_R$$
$$\ell_L = \begin{pmatrix} \nu_e \\ e^- \end{pmatrix}_L, \begin{pmatrix} \nu_\mu \\ \mu^- \end{pmatrix}_L, \begin{pmatrix} \nu_\tau \\ \tau \end{pmatrix}_L$$

The Lagrangian of the EW model introduces three bosons $W_\mu^{(1,2,3)}$ corresponding to $SU(2)$ and one B_μ corresponding to $U(1)$. Th experimentally observed $W^\pm$ are combination of $W_\mu^{(1)}$ and $W_\mu^{(2)}$ whereas photon (A) and the Z-boson are linear combinations of $W_\mu^{(3)}$ and B_μ based on the weak mixing angle (θ_W) as given below:

$$A_\mu = +B_\mu \cos\theta_W + W_\mu^{(3)} \sin\theta_W$$
$$Z_\mu = -B_\mu \sin\theta_W + W_\mu^{(3)} \cos\theta_W$$

The weak interaction for the quark sector can be explained by creating similar $SU(2)$ doublets(Q).

$$Q = \begin{pmatrix} u \\ d' \end{pmatrix}, \begin{pmatrix} c \\ s' \end{pmatrix}, \begin{pmatrix} t \\ b' \end{pmatrix}$$

The strength of the weak interactions for quarks is determined experimentally by studying nuclear β-decay. It is observed that the vertices corresponding to different quark flavours have different coupling strengths. The reason for this is given by the Cabibo hypothesis which states that, the flavour eigen states that participate in the weak interactions are a mixture of the mass eigen states. The relation between them is given by the Cabibo-Kobayashi-Maskawa (CKM) matrix.

$$\begin{pmatrix} d' \\ s' \\ b' \end{pmatrix} = \begin{pmatrix} V_{ud} & V_{us} & V_{ub} \\ V_{cd} & V_{cs} & V_{cb} \\ V_{td} & V_{ts} & V_{tb} \end{pmatrix} \begin{pmatrix} d \\ s \\ b \end{pmatrix}$$

The values of the CKM matrix elements can be found in [1]. The diagonal of the matrix is close to unity, suggesting that the weak interaction is stronger within the same generation of quarks.

The experiments at the Gargamelle bubble chamber in 1973 hinted the evidence of a neutral massive boson responsible for the observed neutrino interactions [2]. In 1983, the Z-boson was directly

discovered at the Super-Proton Synchrotron at CERN. The electroweak theory was verified by this pathbreaking discovery. The properties of the Z-boson were studied at the Large Electron-Positron (LEP) collider at CERN. The discovery of Z and W bosons are among the crucial tests of the Standard Model.

1.3 The Higgs mechanism

1.4 Physics at the hadron colliders

Parton Distribution Functions(PDFs)

Protons at the LHC collide at high energies giving rise to deep inelastic interactions called hard processes. In such cases, the interactions are not between protons but between their constituents which are quarks and gluons, collectively known as *partons*. These partons carry a fraction of the total momentum of the proton (or a hadron in general). In order to study an interaction, it is important to know the effective energy of the interacting partons and their flavour. This information is encoded in the Parton Distribution Functions (PDFs). It describes the probability of finding a parton of certain flavour i, carrying a momentum fraction x_i at a certain energy scale.

Pileup

The primary hard scatter collisions, that are of interest, are contaminated by soft interactions called pileup. It is defined by the average number of interactions recorded per bunch crossing. Sources of pileup are categorized into in-time and out-of-time pileup. In-time pile up is due to collisions occurring in the same bunch-crossing and out-of-time pile-up is contributed by the collisions from previous or later bunches. Some of the sub-detectors have sensitivity windows longer than the interval between bunch crossings. This eventually affects the recorded number of interactions per bunch. The accurate detection of objects under study becomes difficult due to pile-up events. The higher the luminosity, more the pileup. The object reconstruction algorithms have dedicated procedures to mitigate pileup.

Luminosity and cross-section (σ)

The quantity that measures the ability of a collider to produce particle interactions is called instantaneous luminosity ($\mathcal{L}$). The instantaneous luminosity integrated over the lifetime of collider operation is called integrated luminosity (L).

In order to define the event rate for interesting processes, along with luminosity, we require another quantity called the cross-section. At the subatomic scale, the particle interactions are governed by laws of quantum physics. Therefore, a theory can predict the *probablility* of certain outcomes of collisions. The probablity that a certain process will take place is called its cross-section (σ). Finally, the number of event rate of specific interactions is defined as the product of integrated luminosity and the cross-section (Eq. (1.1)).

$$R = \sigma \cdot \int_{dt} \mathcal{L}(t) \tag{1.1}$$

For a particle collider, beam energies and the luminosity are two important figures of merit. High energy allows the production of new heavy particles and high luminosity allows more flux of particles contributing to high number of collisions.

Lepton universality..because tZq trilepton, decay into muons and electrons equal probability

branching ratio

1.5 Top quark physics

The top quark was discovered in 1995 at the Tevatron laboratory(?) by the CDF collaboration[CITE]. It is the heaviest fundamental particle discovered so far with a mass of 173 GeV[CITE PDG] and since it is close to the EW scale, the top quark might play an important role in understanding Electroweak Symmetry Breaking (EWSB). Moreover, the fact that m_t is greater than m_H hints whether the top quark gets its mass through Higgs mechanism.

The top quark is the weak isospin partner of the bottom quark and thus completes the three generation structure of the SM. Since its discovery, top quark has been a crucial part of any physics program at the hadron colliders because of its heavy mass. It decays almost exclusively into W and b before hadronisation. This property gives us a unique opportunity to study a "bare" quark because some top quark properties are conserved in the decay process and passed on to its decay products.

The LHC is a top factory becuase it can produce abundant top quarks and other related processes. Therefore, LHC provides a lot of data which is analysed extensively to understand the top quark and its properties. The production of top quarks is mainly through three kinds of processes: Wt-channel, t-channel and the s-channel.

CHAPTER 2

Signal Extraction and Background Processes

The chapter provides a detailed description about the tZq process and its trilepton decay channel which is the signal in this analysis. The baseline event selection defined to extract maximum signal is given in Section 2.2.1. The different background processes are described in Section 2.3. In addition, information about Monte Carlo simulated samples for signal and background processes can be found in Section 2.4. The various sources of systematic uncertainties are outlined in Section 2.6. Moreover, a brief explanation of neural networks is also provided at the end.

2.1 The tZq production

Since at the LHC, high energies are attainable by particles, production of heavy particles such as the t-quark and its related processes, become highly probable. For this reason, LHC is called a top factory. One of the rare processes at the LHC is the associated production of the t-quark and the Z-boson through electroweak interactions. It is referred to as the tZq production. Its LO t-channel Feynman diagrams are shown in Fig. 2.1. A Z-boson is radiated from any one of the incoming or outgoing quarks (Fig. 2.1(a)) or from the exchanged W-boson (Fig. 2.1(b)). In addition to these resonant contributions, there is also a small non-resonant contribution in the form of tl^+l^-q (Fig. 2.1(c)) which is also accounted for in this analysis. The associated t-quark is produced through interactions such as $u + b \rightarrow d + Z + t$ or $\overline{u} + b \rightarrow \overline{d} + Z + t$ whereas $\bar{t}$-quark is produced via the charge conjugate processes.

The tZq production is interesting to study because it probes the coupling of t and Z as well as the WWZ coupling. In other words, it allows the coupling of two bosons and the coupling of a fermion to a boson to be studied in a single interaction. Moreover, it can provide a solid basis to study similar processes such as the tHq process. The theoretical cross-section based on SM prediction is calculated at NLO in QCD for a dilepton mass more than 30 GeV, is $(102\,^{+5}_{+2})$ fb. The tZq process was observed by ATLAS and CMS during the Run-2 of the LHC. The cross-section, measured by the ATLAS collaboration, is $(97 \pm 13\,(\text{stat.}) \pm 7\,(\text{sys.}))$ fb [3] which is consistent with the SM expectation.

In order to study this process, one has to note that the particles involved are quite heavy and therefore, the only way to spot them is from their reconstructed decay products. Moreover, depending on the branching ratio, there can be several sets of final states. A common practice is to divide the possible final states into *channels* based on certain combinations of leptons and jets. This analysis focuses on the so-called trilepton channel which is described below.

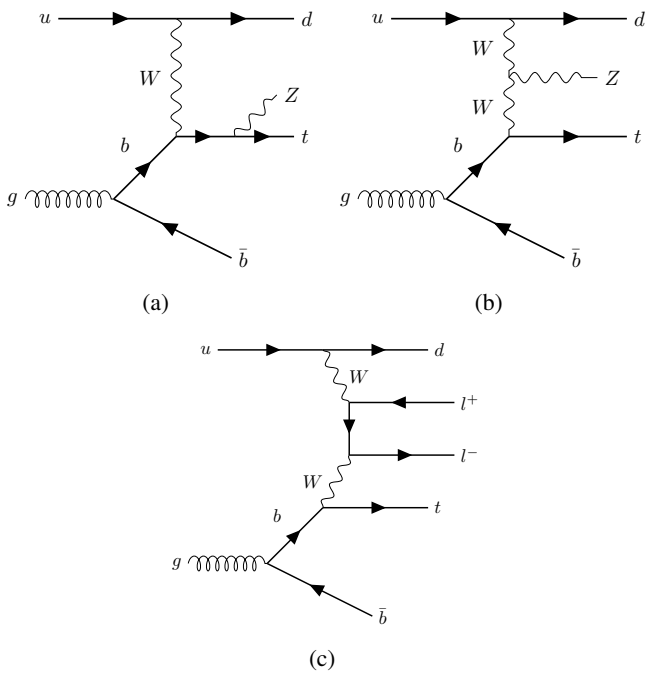

Figure 2.1: Feynman diagrams at LO for the tZq-production. The Z is radiated either from one of the quarks or from the exchanged W boson.

2.2 The tZq Trilepton Channel

As the name suggests, the trilepton decay channel of the tZq production contains final states with three charged leptons, as shown in Fig. 2.3. The t-quark decays almost exclusively into b W and the corresponding W can decay either leptonically or hadronically. Approximately in 25% events, W decays into a charged lepton and an associated neutrino. The Z-boson can decay either into a pair of leptons or into neutrinos (invisible) or into hadrons. In approximately 8% of the produced events, the Z boson decays into opposite sign same flavour lepton pairs. Its probability is equal across the three lepton families (e^-,μ^-,τ^-) owing to lepton universality. This analysis includes Z decays resulting into electrons or muons (e^- e^+ or μ^- μ^+). The tau leptons are considered if they decay into lighter leptons (i.e. e^- or μ^-).

The branching fractions of the various possible decays of t and Z is shown in Fig. 2.2. The combination of both t and Z decaying into leptons occurs in only 2% of the produced tZq events. However, selecting the trilepton decay state has its advantages. First and foremost, the efficiency of reconstructing leptons is higher than that of hadrons because of the clean signatures of leptons. In addition, a decay state with three leptons is difficult to replicate by background processes which ensures signal purity. Due to these reasons, the trilepton channel is chosen for studying the tZq process. From this point onward, this will be referred to as the signal.

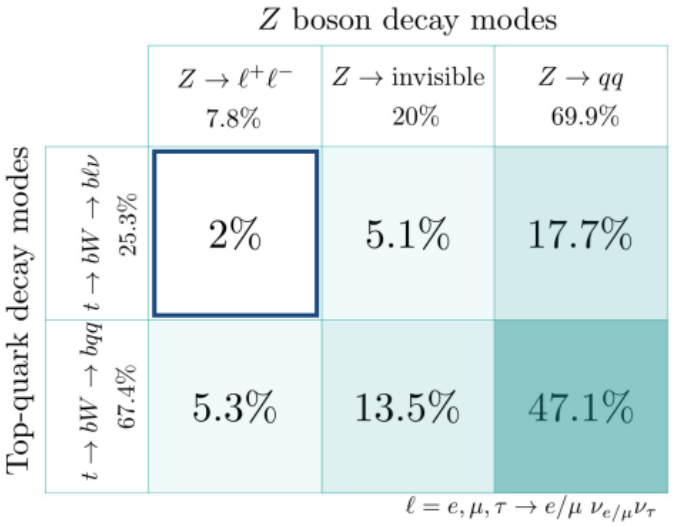

Figure 2.2: Branching ratios of possible decays of t and Z, along with the fractions representing combination of decays [4]

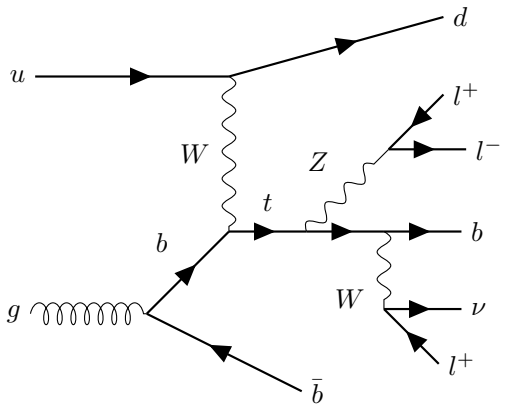

Figure 2.3: The *tZq* trilepton final state

2.2.1 Event Selection

In LHC physics, the outcome of a collision between two incoming particles is called as an "event". An important step in an analysis is to reconstruct the final state of interest from the detector data or in other words, find possible occurrences of this final state within the collision events. In order to achieve that, certain requirements are defined in favour of the signal events. The collection of these requirements is called event selection. For this analysis, the primary event selection is discussed below and summarised in Table 2.1.

- **Leptons**
  - Exactly three leptons (e^- or μ), τ is considered if it decays into leptons. These leptons are sorted by their p_{T} which is required to be at least 27,15 and 10 GeV, respectively.
  - At least 1 Opposite Sign Same Flavour (OSSF) lepton pair with a minimum difference between its invariant mass (m_{ll}) and m_Z. This is to identify which out of the selected leptons originate from Z.
  - A cut on minimum accepted invariant mass, in order to suppress backgrounds not containing a Z.
  - A cut on the transverse mass of the W-boson is applied to account for the missing transverse energy.
- **Jets**
  - Number of jets are required to be between 2 and 5, with p_{T} more than 25 GeV and $|\eta|$ more than 4.5.
  - Number of b-jets are required to be 1 or 2, reconstructed at 85% working point with $|\eta|$ more than 2.5. Events with 2 jets, both b-tagged are not considered.

Table 2.1: Event selection

Variable	Preselection
N_ℓ $(\ell = e, \mu)$	= 3
	≥ 1 OSSF lepton pair
p_{T} (ℓ_1, ℓ_2, ℓ_3)	> 27, 15, 10 GeV
$\min(m_{\ell\ell})$	> 20 GeV
$\lvert m_{\ell\ell} - m_Z \rvert$	< 10 GeV
$m_{\mathrm{T}}(\ell, E_{\mathrm{T}}^{\mathrm{miss}})$	> 30 GeV
N_{jets} $(p_{\mathrm{T}} > 25$ GeV)	2-5
$N_{b-\mathrm{jets}}$@85%	1-2 (no $2j2b$)

It is important to note here that these requirements are chosen to maximise the probability of selecting signal events but in reality there are background processes that mimic the tZq signature and therefore, contaminate the selected signal events.

2.3 Background processes

The background processes for tZq process can be classified according to the number of prompt (or real) leptons in the final state. A lepton is labelled prompt if it originates from either a τ or a massive boson. On the other hand, non-prompt or fake leptons are objects misidentified as leptons. The source of non-prompt leptons can be bottom and charm hadron decays, meson decays, photon conversions or light jets creating lepton-like signatures. Backgrounds involving only prompt leptons are diboson, $t\bar{t}$+X, $t\bar{t}H$ and tWZ while backgrounds involving non-prompt leptons are $t\bar{t}$, Z +jets and tW.

Backgrounds involving prompt leptons

In the diboson process, two massive bosons are produced which can be ZZ, WW or WZ, as shown in Fig. 2.4. As per Fig. 2.4(a), the leptonic decay of bosons result into three prompt leptons which can pass the signal event selection if additional jets are also found. For the ZZ scenario, as shown in Fig. 2.4(b), one of the leptons needs to fail the requirement for a prompt lepton or is not reconstructed. Due to this strong resemblance of the diboson signature with the signal, it is the dominant background in the tZq production.

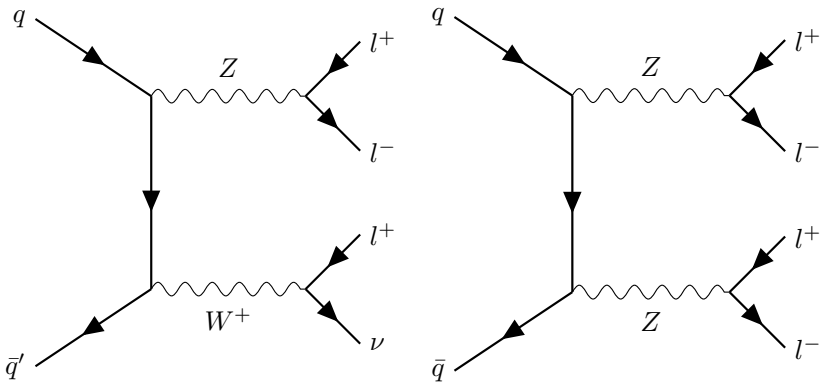

Figure 2.4: Feynman diagrams for the diboson background

The t-quark pair production in association with a heavy boson (Z or W) can be an important source of background. In particular, the $t\bar{t}Z$ process, where the final state already includes a Z boson and a t quark, can produce a very similar signal-like signature. It is shown in Fig. 2.5. The $t\bar{t}H$ contributes less because of its small cross-section.

Backgrounds involving non-prompt leptons

Backgrounds involving non-prompt or fake lepton are t-quark pair production and the production Z-boson with jets. As shown in Fig. 2.6(b), there are already two leptons from the Z-boson. If the jets are light, they can be misidentified as leptons leading to a non-prompt lepton contribution. In the $t\bar{t}$ production, as shown in Fig. 2.6(b), if one of the b-jet decays into a lepton, then it can satisfy the signal event selection.

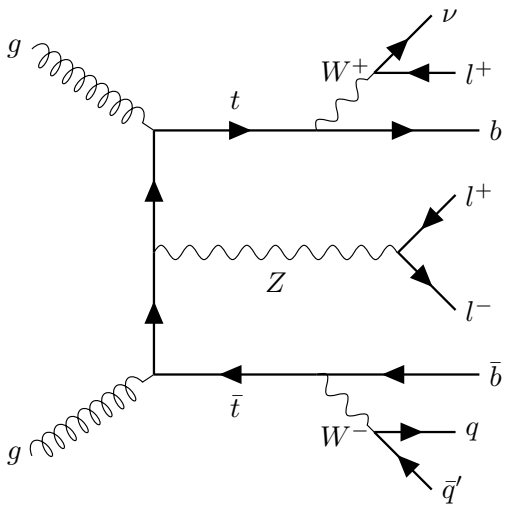

Figure 2.5: Feynman diagrams for the $t\bar{t}Z$ background

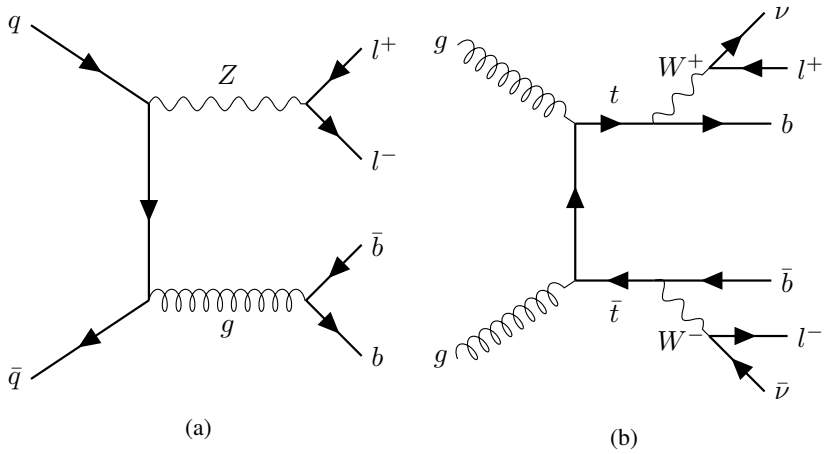

Figure 2.6: Feynman diagrams for non-prompt lepton background

2.4 Monte-Carlo (MC) simulations

As already discussed before, proton-proton collisions are viewed as collisions between partons. This is not a simple process because multiple interactions can occur within the same event. With this complexity, it becomes difficult to study the interaction of interest and more importantly the task of segregating signal from background becomes more complex. Here is where, Monte Carlo generators come to the rescue. Monte Carlo generators are software that simulate collision events and try to provide a detailed description of the possible final states. In addition, these generators, also called event generators, can also simulate detector response. In practice, the generators use pseudo-random numbers to reproduce the quantum mechanical probabilities of different outcomes for a collision event [5].

The simulated data provided by these generators can be thought of as a "digital twin" of the actual observed data. It can be used to predict any experimental observable or a combination of observables. The workflow of MC generators, called as the MC chain, is a step-by-step process that begins with identifying the hard interaction and continues until the final state is achieved. At each stage, the structure of the underlying event evolves. The steps are briefly summarised below:

- **Hard process**: In this step the hard process, defined as the process with the highest momentum transfer, is determined using matrix element calculation combined with the input Parton Distribution Functions. If a resonance is produced in a hard process, such as the t or Z and it shortly decays, then its decay process is also considered within the hard process.
- **Parton Shower (PS)**: The colliding partons are responsible for emissions that give rise to more partons and subsequently more interactions. The emissions associated with the incoming partons is called Initial-State Radiation (ISR) while the emissions associated with the outgoing partons is called Final-State Radiation (FSR). These emissions and their respective interactions are modelled with Parton Shower algorithms. The incorporation of PS into the matrix element paints a more accurate picture of the collision process.
- **Multiple-processes**: Until now, only one of the partons from the original hadron is considered but in reality, other partons from the same hadron also interact. Their interactions are termed as multiple-processes. They are calculated at this step of the MC simulation chain.
- **Hadronisation and decay**: The outgoing partons, with sufficient energy, can produce new hadrons due to QCD colour confinement (hadronisation). If these hadrons are unstable, they can also decay into lighter particles. The MC chain also includes these calculations.

After all the MC events are generated, the interactions of the particles with the detector material is simulated using the GEANT4 software toolkit [6]. Finally, the simulated data is ready for comparison with the observed detector data. The workflow of the MC chain is illustrated in Fig. 2.7. Among the various available MC generators, Herwig [7] and Pythia [8] are two of the most commonly used ones.

2.5 Data and simulated samples

This analysis uses collision data collected by the ATLAS detector during 2015 to 2018 (Run-2 of the LHC) at a center of mass energy of 13 GeV. The total integrated luminosity is of 140.1 fb^{-1}.

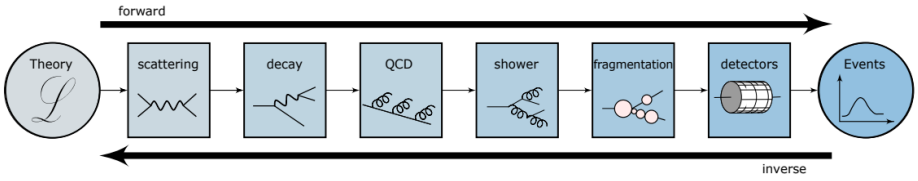

Figure 2.7: An illustration of the steps involved in a Monte Carlo chain [9]

The ATLAS MC samples for analysis of the Run-2 dataset are divided into three subsets: `mc16a` generated with 2015 an 2016 pileup conditions, `mc16d` generated with 2017 pileup conditions and `mc16e` that includes pileup conditions of 2018 data.

2.5.1 Signal sample

The *tZq* signal sample is simulated using MadGraph5_aMC@NLO 2.9.5 generated at next-to-leading order (NLO) with NNPDF3.0NLO parton distribution function. In general, the models used for PS and hadronisation contain several free parameters which must be optimised to generate a reasonable description of data. The optimisation is termed as tuning and the resulting sets of parameters are called tune sets. For the signal sample, Pythia 8.245 is used for Parton Shower and hadronisation along with A14 (ATLAS 24 [10]) tune set and the NNPDF2.3LO PDF set. The *t*-quark is decayed at LO using MADSPIN.

UPDATE THIS AFTER NEW SAMPLE and add info about scales

2.5.2 Background samples

For the background processes, different versions of MadGraph5_aMC@NLO [11], Sherpa [12] or Powheg [13] generators are used to calculate the matrix element and cross-sections combined with the NNPDFx.xNLO PDF set. The PS and hadronisation is modeled with Pythia for the nominal background samples and Herwig for the alternate sample generation. The alternate samples are required for the theoretical uncertainties as described in SECTION. The specific versions used for different backgrounds is summarised in Table 2.2.

Add the detailed DSIDs and everything in the appendix and refer here

2.6 Systematic Uncertainties

One of the key advantages of using simulated data is their ability to predict how the observed data may appear. However, it is crucial to assess how dependable both the simulated and the measured data are, which is quantified through uncertainties. The proper inclusion of uncertainties is an important part of any analysis.

Uncertainties can be divided into two sections: statistical and systematic. Simply put, statistical uncertainties are related to the statistics of the data whereas systematic uncertainties are complex uncertainties that are not directly from the statistics of the data. For instance, the length of an object is

Table 2.2: Background sample details

Background	Generator	Parton Shower	PDF	Type of Sample
$t\bar{t}Z$	MadGraph5_aMC@NLO 2.8.1	Pythia 8.244	NNPDF3.0NLO NNPDF2.3LO	Nominal
$t\bar{t}Z$	MadGraph5_aMC@NLO 2.8.1	Herwig 7.2.1	NNPDF3.0NLO NNPDF2.3LO	Alternate
tWZ	MadGraph5_aMC@NLO 2.X.X	Pythia 8.235	NNPDF3.0NLO	Nominal
Diboson	Sherpa 2.2.12	Sherpa MEPS@NLO	NNPDF3.0NNLO	Nominal
Triboson	Sherpa 2.2.2	Sherpa MEPS@NLO	NNPDF3.0NNLO	Nominal
$t\bar{t}$	Powheg Box v2	Pythia 8.230	NNPDF3.0NLO NNPDF2.3LO	Nominal
$t\bar{t}$	Herwig 7.2.1	Pythia 8.230	NNPDF3.0NLO	Alternate
tW	Powheg Box v2	Pythia 8.230	NNPDF3.0NLO NNPDF2.3LO	Nominal
Z+ jets	Sherpa 2.2.11	Sherpa MEPS@NLO	NNPDF3.0NNLO	Nominal
$t\bar{t}W$	Sherpa 2.2.10	Sherpa MEPS@NLO		Nominal
$t\bar{t}H$	Powheg Box v2	Pythia 8.230	NNPDF3.0NLO NNPDF2.3LO	Nominal
$t\bar{t}t$	MadGraph5_aMC@NLO 2.2.2	Pythia 8.186	NNPDF2.3LO	Nominal
$t\bar{t}t\bar{t}$	MadGraph5_aMC@NLO 2.3.3	Pythia 8.230	NNPDF3.1LO	Nominal
$t\bar{t}t\bar{t}$	MadGraph5_aMC@NLO 2.3.3	Herwig 7.0.4	NNPDF3.1LO	Alternate

measured with a ruler and is found to be 10 ± 0.5 cm. Here the statistical uncertainty is 0.5 cm. In addition, there is a systematic uncertainty which can originate from the calibration of the ruler.

In high energy physics, sources of systematic uncertainties are calibrations of scales, efficiencies of particle identifications and reconstructions, choice of MC generators, etc. These sources of systematic uncertainties are categorised into: instrumental and theoretical uncertainties as described in Section 2.6.1 and Section 2.6.2, respectively.

2.6.1 Instrumental or detector uncertainties

- **Luminosity**: The integrated luminosity is 140.1 $fb^{-1}$and the uncertainty in its calculation is 0.83%
- **Pileup reweighting**: MC generators make use of scale factors to account for differences in pileup distributions between data and simulations. There is an uncertainty associated with these scale factors. It is evaluated by changing the nominal pileup value to a lower and a higher value, then the effect of these changes is calculated to obtain the up and down uncertainty.
- **Jet Energy Scale (JES)**: After the jets are reconstructed, their energies need to be adjusted so that it reflects the energy of the colliding particles. The calibration is done by comparing the reconstructed jets with the true jets which are simulated jets of stable particles without detector effects. Uncertainties originating from the calibration process are categorised as JES uncertainties [14].
- **Jet Energy Resolution (JER)**: JER is the detector's ability to distinguish two jets with similar total energy. The uncertainty associated with the differences in JER in case of data and simulation is called JER uncertainty.

- **Jet-Vertex-Tagger (JVT)**: It is a discriminant in the form of likelihood constructed using track-based variables, sensitive to the origin of jets. A cut is applied on the JVT factor to reject jets coming from pileup [15]. The uncertainty associated with the JVT factor is one of the systematics.

- **Lepton reconstruction**: Scale factors are applied to correct differences between data and simulation in case of lepton identification, isolation and trigger efficiencies. The uncertainties associated with these scale factors belong to the lepton reconstruction category of systematics.

2.6.2 Theoretical uncertainties

This category involves uncertainties originating from the various models used in the MC simulation chain, and therefore, also called modeling uncertainties or modeling systematics. There are various parameters related to the modelling of a certain process and for each parameter, there is an associated uncertainty which is investigated by varying the values of the parameters. The effect of the variation is estimated and assigned as the systematic uncertainty. In this way, the uncertainties associated with the modelling of the process is extracted.

- **A14**: The uncertainty associated with the A14 tune set is determined by comparing the nominal sample with two alternate samples, both simulated using the same settings as the nominal sample but incorporating the up and down variations of the A14 tune set. This variation is related to the strong coupling constant α_s. This uncertainty is considered for tZq and $t\bar{t}Z$ processes.

- **Scale**: The parameters representing renormalisation and factorisation scales are known as μ_R and μ_F, respectively and their values are μ_R=μ_F=$H_T/6$. The renormalisation scale is for the running of α_S associated with the hard process whereas the factorisation scale for the PDFs. They are introduced to prevent the matrix element from any possible divergences. In order to estimate the uncertainty on the parameters, the values of μ_R and μ_F are varied between μ_R=μ_F=0.5, μ_R=μ_F=1 and μ_R=μ_F=2. This uncertainty is considered for tZq, diboson and $t\bar{t}Z$ processes.

- **Shower and PDF**: The showering uncertainty is calculated by comparing the nominal sample (modeled using Pythia) and the alternate sample (modeled using Herwig). Moreover, uncertainty associated with the PDF is also considered. The shower systematic is included for tZq, $t\bar{t}Z$ and $t\bar{t}$ processes whereas the PDF uncertainty is considered for tZq, diboson and $t\bar{t}Z$ processes.

write about pdf4lhc

- **Interference**: This uncertainty accounts for the interference between $t\bar{t}Z$ and tWZ processes. The non-resonant tWZ production can feature a resonant $\bar{t}$ in the intermediate state, leading to overlap with the $t\bar{t}Z$ production. This interference is navigated using various techniques called diagram removal (DR) and diagram subtraction (DS). Two tWZ samples were generated, one with DR1 and another with DR2 and the difference is taken to be the tWZ modeling uncertainty.

- **Matrix element matching and resummation**: The systematics in this category are taken into account for the diboson process following the recommendations of the Physics Modelling Group [16, 17]. The CKKW parameter is related to the calculation of the overlap between jets involved in the matrix element and parton shower computation. The nominal value of the

parameter CKKW is 20 GeV and its uncertainty is estimated by varying this value to 30 GeV (up variation) and 15 GeV (down variation) [18]. The QSF parameter determines the scale for the resummation of soft gluon emissions. Its uncertainty is estimated by varying the nominal by 2 and 0.5 [18].

In the parton shower computation, a recoil scheme refers to how the remaining partons adjust their momenta after emission or splitting, in order to conserve the total momentum. The recoil scheme used for the diboson samples is described in [19]. The uncertainty on the associated parameter CSSKIN is also considered for the diboson process. Finally, approximate NLO EW corrections are included as weights using the electroweak virtual approximation as described in [20].

- **Matching and ISR**: The $t\bar{t}$ background is being modelled using POWHEG generator in which a parameter called h_{damp} is the damping factor that controls the radiation at which the $t\bar{t}$ system recoils. If this is set to infinity then all the radiation is considered in the computation of ISR. The uncertainty on ISR is estimated by comparing two nominal $t\bar{t}$ samples, one with h_{damp}=1.5m_t and second with h_{damp}=3m_t.

  Depending on the generator and parton shower workflow, there might be overlapping phase spaces which can cause double-counting of events. To prevent this, a parameter called PTHARD is defined which refers to the hard scattering transverse momentum scale. This parameter decides the extent of phase space which is vetoed while matching matrix element with the parton shower. The uncertainty on PTHARD is estimated by comparing samples with PTHARD=1 and PTHARD=0.

2.7 Event weights

The events generated from the Monte Carlo simulation are unweighted, which means that each event represents an equal share of the total cross-section. However, for obtaining a correct distribution of an observable, each raw event is required to be weighted. Generally, these weights are provided by the MC generator.

The nominal event weight (w_{MC}) is the measure of the relative probability of an event within a sample. Along with the nominal weight, there are other weights representing parameter or setting variations associated with systematic uncertainty estimation. Consider a systematic which requires a parameter to be varied. Now, producing the entire event sample with the varied parameter is computation intensive. Instead, a corresponding weight is included in the event generation [21]. The total sum of these weights give the corrected number of events for that sample.

The total event weight can be written as:

$$w_{\text{total}} = w_{\text{MC}} \cdot w_{\text{pileup}} \cdot w_{\text{lepton}} \cdot w_{\text{JVT}} \cdot w_{\text{trigger}} \cdot w_{b\text{-tagging}} \tag{2.1}$$

- w_{MC}: gives the relative probability of producing that event
- w_{pileup}: to correct the pileup profile of simulated events to match observed data
- w_{lepton}: to correct for the differences in lepton isolation and reconstruction between MC and data

- w_{JVT}: differences in data and MC when applying a cut on the JVT factor are considered by applying this weight
- w_{trigger}: any inconsistency between data and MC related to trigger efficiencies is corrected with this weight
- $w_{b\text{-tagging}}$: this analysis requires events to contain b-jets. This is ensured by a applying a weight called $w_{b\text{-tagging}}$

2.8 Artificial Neural Networks

A neural network is a computation tool developed to function in a way similar to the human mind. It is widely used in high energy physics for data analysis. The structure of a neural network (NN) is made up of neurons or *nodes*. Their function is to examine unknown systems and identifying interesting features, just like the job of neurons in human mind. Generally, these nodes are arranged in three different layers: the input layer, the hidden layer and the output layer. A list of variables is given as input to the nodes of the input layer. Processing takes place through the subsequent layers and at the end, the output layer returns the conclusions derived by the network. Connections between nodes of different layers are referred to as the *synapses*. Each connection between nodes of two consecutive layers, has a weight associated to it. Figure 2.8 shows a diagram of a neural network.

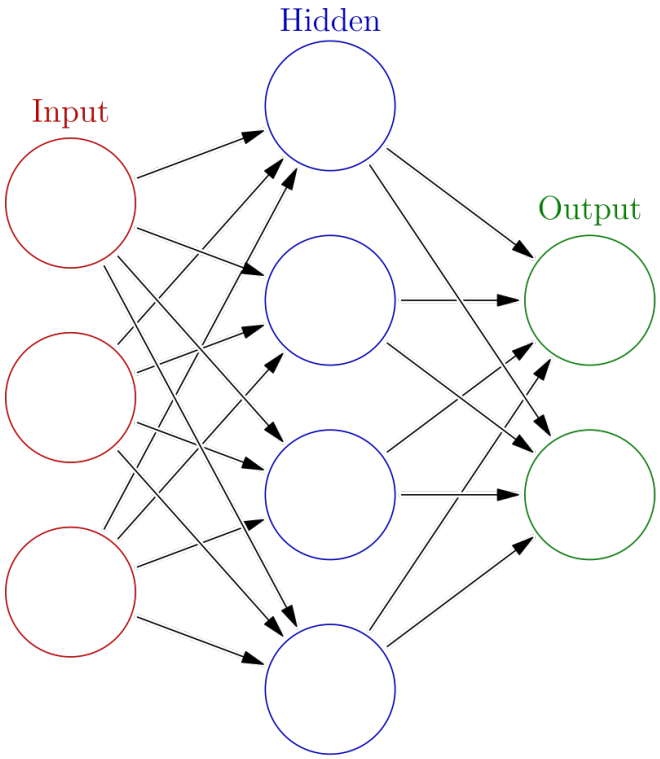

Figure 2.8: Diagram of a neural network including the input, hidden and output layers [22]

The input received by each node is the sum of weighted output of all nodes of the previous layer. As given in Equation 2.2, y_j is the input to node j, w_{ij} is the weight from the i-th node and x_i is that node's output. The term w_{0j} is called bias.

$$y_j = \Sigma_{i=1}^{n} w_{ij} x_i + w_{0j} \tag{2.2}$$

The output of a node is defined by an *activation* function. Common choice of an activation function is the sigmoid function. It provides output between 0 and 1. A feature that makes a NN special is its capability to *learn* from examples with known inputs and outputs. This is referred to as *training* a neural network. The purpose of training is to find appropriate weights. In supervised training, inputs and outputs are provided to a NN. It processes input and then compares the resultant output with the desired output. Comparison is done by calculating a *loss function*. It is a way to determine how well is the network trained. For better performance of a network the loss function should be minimised. In order to do that, errors of the resultant output are propagated back in a model and the initial weights are readjusted so that output is closer to the desired output. This is how a network learns. A dataset flows inside a network several times and each time weights are refined until a minimum value of the loss function is obtained.

Bibliography

[1] S. N. et al. (Particle Data Group), Phys. Rev. D 110, 030001 (2024), URL: https://pdg.lbl.gov/2024/api/index.html (cit. on p. 3).

[2] F. Hasert et al., *Observation of neutrino-like interactions without muon or electron in the gargamelle neutrino experiment*, Physics Letters B **46** (1973) 138, ISSN: 0370-2693, URL: https://www.sciencedirect.com/science/article/pii/0370269373904991 (cit. on p. 3).

[3] *Observation of the associated production of a top quark and a Z boson in pp collisions at $\sqrt{s}$= 13 TeV with the ATLAS detector*, Journal of High Energy Physics **2020** (2020) 124, URL: https://doi.org/10.1007/JHEP07(2020)124 (cit. on p. 7).

[4] I. A. Cioara, *Associated Production of a Top Quark and a Z Boson in pp Collisions at $\sqrt{s}$ = 13 TeV Using the ATLAS Detector*, BONN-IR-2018-07, PhD Thesis: University of Bonn, 2018, URL: https://hdl.handle.net/20.500.11811/7636 (cit. on p. 9).

[5] T. Sjöstrand, *Monte Carlo Generators*, 2006 European School of High-Energy Physics, ESHEP 2006 (2006) (cit. on p. 13).

[6] S. Agostinelli et al., *GEANT4–a simulation toolkit*, Nucl. Instrum. Meth. A **506** (2003) 250 (cit. on p. 13).

[7] J. Bellm et al., *Herwig 7.0/Herwig++ 3.0 release note*, The European Physical Journal C **76** (2016) 196, URL: https://doi.org/10.1140/epjc/s10052-016-4018-8 (cit. on p. 13).

[8] T. Sjöstrand, S. Mrenna and P. Skands, *A brief introduction to PYTHIA 8.1*, Computer Physics Communications **178** (2008) 852, ISSN: 0010-4655, URL: https://www.sciencedirect.com/science/article/pii/S0010465508000441 (cit. on p. 13).

[9] T. Plehn et al., *Modern Machine Learning for LHC Physicists*, (2022), arXiv: 2211.01421 [hep-ph] (cit. on p. 14).

[10] *ATLAS Pythia 8 tunes to 7 TeV data*, tech. rep., All figures including auxiliary figures are available at https://atlas.web.cern.ch/Atlas/GROUPS/PHYSICS/PUBNOTES/ATL-PHYS-PUB-2014-021: CERN, 2014, URL: https://cds.cern.ch/record/1966419 (cit. on p. 14).

[11] J. Alwall et al., *The automated computation of tree-level and next-to-leading order differential cross sections, and their matching to parton shower simulations*, JHEP **07** (2014) 079, arXiv: 1405.0301 [hep-ph] (cit. on p. 14).

[12] T. Gleisberg et al., *Event generation with SHERPA 1.1*, Journal of High Energy Physics **2009** (2009) 007, URL: https://dx.doi.org/10.1088/1126-6708/2009/02/007 (cit. on p. 14).

[13] A. Banfi et al., *A POWHEG generator for deep inelastic scattering*, JHEP **02** (2024) 023, arXiv: 2309.02127 [hep-ph] (cit. on p. 14).

[14] T. Barillari and O. behalf of the ATLAS Collaboration, *Jet Energy Scale Uncertainties in ATLAS*, Journal of Physics: Conference Series **404** (2012) 012012, URL: https://dx.doi.org/10.1088/1742-6596/404/1/012012 (cit. on p. 15).

[15] *A new tagger for the charge identification of b-jets*, (2015) (cit. on p. 16).

[16] ATLAS Internal, *Physics Modelling Group*, 2024, URL: https://twiki.cern.ch/twiki/bin/view/AtlasProtected/PhysicsModellingGroup (cit. on p. 16).

[17] ATLAS Internal, *Weak Boson Processes*, 2024, URL: https://twiki.cern.ch/twiki/bin/view/AtlasProtected/PmgWeakBosonProcesses (cit. on p. 16).

[18] J. K. Anders and M. D'Onofrio, *V+Jets theoretical uncertainties estimation via a parameterisation method*, tech. rep., CERN, 2016, URL: https://cds.cern.ch/record/2125718 (cit. on p. 17).

[19] S. Schumann and F. Krauss, *A Parton shower algorithm based on Catani-Seymour dipole factorisation*, JHEP **03** (2008) 038, arXiv: 0709.1027 [hep-ph] (cit. on p. 17).

[20] S. Kallweit, J. M. Lindert, P. Maierhöfer, S. Pozzorini and M. Schönherr, *NLO electroweak automation and precise predictions for W + multijet production at the LHC*, Journal of High Energy Physics **2015** (2015) 12, URL: https://doi.org/10.1007/JHEP04(2015)012 (cit. on p. 17).

[21] C. Bierlich et al., *A comprehensive guide to the physics and usage of PYTHIA 8.3*, SciPost Phys. Codebases (2022) 8, URL: https://scipost.org/10.21468/SciPostPhysCodeb.8 (cit. on p. 17).

[22] *Artificial Neural Network*, Accessed on: 26.09.2024, URL: https://en.wikipedia.org/wiki/Artificial_neural_network (cit. on p. 18).

List of Figures

List of Tables